The efficacy of laser material processing for enhancing stem cell adhesion and growth on different materials

David Waugh and Jonathan Lawrence

Author post-print (accepted) deposited by Coventry University's Repository

Original citation & hyperlink:

Waugh, D. G., and J. Lawrence. "The Efficacy of Laser Material Processing for Enhancing Stem Cell Adhesion and Growth on Different Materials." *Advances in Contact Angle, Wettability and Adhesion* 3 (2018): 373-397.
https://dx.doi.org/**10.1002/9781119459996.ch16**

ISBN 9781119459941

Publisher: Wiley

This is the peer reviewed version of the following article: Waugh, D. G., and J. Lawrence. "The Efficacy of Laser Material Processing for Enhancing Stem Cell Adhesion and Growth on Different Materials." *Advances in Contact Angle, Wettability and Adhesion* 3 (2018): 373-397**, which has been published in final form at** https://dx.doi.org/**10.1002/9781119459996.ch16. This article may be used for non-commercial purposes in accordance with Wiley Terms and Conditions for Self-Archiving.**

The full publication in which this chapter appears is available online at:
https://www.wiley.com/en-gb/Advances+in+Contact+Angle%2C+Wettability+and+Adhesion%2C+Volume+3-p-9781119459958.

Copyright © and Moral Rights are retained by the author(s) and/ or other copyright owners. A copy can be downloaded for personal non-commercial research or study, without prior permission or charge. This item cannot be reproduced or quoted extensively from without first obtaining permission in writing from the copyright holder(s). The content must not be changed in any way or sold commercially in any format or medium without the formal permission of the copyright holders.

This document is the author's post-print version, incorporating any revisions agreed during the peer-review process. Some differences between the published version and this version may remain and you are advised to consult the published version if you wish to cite from it.

*Corresponding Author: david.waugh@coventry.ac.uk

The efficacy of laser material processing for enhancing stem cell adhesion and growth on different materials

D.G. Waugh* and J. Lawrence

School of Mechanical, Aerospace and Automotive Engineering, Faculty of Engineering, Environment and Computing, Coventry University, Gulson Road, Coventry CV1 2JH, UK.

Abstract

The need for more efficient and effective stem cell therapies and technologies is ever increasing on account of a general ageing worldwide population, leading to a number of competing techniques to provide an effective means for the surface engineering of biomaterial substrates, especially in the stem cell technologies arena. This chapter will introduce the role of laser material processing, particularly laser surface engineering, in the field of stem cell research and will show how laser material processing of polymers and metals can modulate the adhesion, growth and proliferation of mesenchymal stem cells (MSCs). Through CO_2 laser surface engineering of polytetrafluoroethylene (PTFE) and polyamide 6,6 it will be shown that the modification of wettability and adhesion characteristics gave rise to an enhanced MSC adhesion and growth. Fibre laser welding of NiTi alloy is demonstrated as giving rise to an enhanced biocompatibility, augmenting MSC adhesion and growth. The efficacy of laser material processing as a means to produce optimized platforms to increase biological adhesion and growth has been shown as viable, indicating that laser material processing has the potential to have a large influence upon the future of biomaterial science and regenerative medicine.

Keywords: Surface engineering, laser, stem cells, bioengineering, adhesion.

1. Introduction

It is well known that many developed countries have issues relating to ageing populations [1,2]. Of major concern are the number of negative economic and health implications which need to be adequately addressed. One field that shows significant promise to counter these negative implications is that of stem cell technologies [3-6]. This is owed to the fact that the nature of mesenchymal stem cells (MSCs) to differentiate into specific cell types (for example osteoblasts and chondrocytes, etc.) [7] makes them critical for the development of biological tissues, making them an ideal candidate for use within the field of regenerative medicine [2,7-11]. What is more, a number of important works have been carried out to show that biological cells [12-14], including MSCs [4,15,16] hold the ability to distinguish between variations in surface characteristics (such as roughness, for example), giving rise to a highly modulated biological cell growth response including variations in adhesion, protein adsorption, differentiation and proliferation. It has been suggested that the use of surface engineering technologies, to assist in the development of substrates to provide a biomimetic environment, offers a substantial approach to enhance and prolong the *in vitro* lifecycle of MSCs whilst still upholding the MSC's multipotency [9,17].

There are many applications of polymers in the biomaterial industry [18-20], as shown in Table 1. The advances in manufacturing and surface engineering techniques have led to many polymeric materials seeing increased use in both the biomedical industry and research. This is due to the fact that clinicians and researchers have an enhanced ability to augment the biocompatibility and biofunctionality of polymeric biomaterials [20,21].

*Corresponding Author: david.waugh@coventry.ac.uk

Table 1: Common applications for polymers within the biomedical industry.

Material	Applications
Polyamide 6,6	Gastrointestinal segments; Tracheal tubes.
Polyethylene (PE)	Acetabular cup of hip prosthesis; heart pacemakers.
Poly(methyl methacrylate) (PMMA)	Dental restorations; intraocular lenses; joint replacement.
Polypropylene	Cardiovascular applications.
Polytetrafluoroethylene (PTFE)	Cardiovascular applications; soft tissue implants; medical devices; medical filtration.
Polyurethane	Heart pacemakers; maxillofacial prosthesis;
Poly(vinyl chloride) (PVC)	Gastrointestinal segments; maxillofacial prosthesis.
Ultrahigh molecular weight polyethylene (UHMWPE)	Total joint replacement- usually hip, knee and shoulder joints.

Another material that has received increasing attention from the biomaterial industry is NiTi alloy. This is attributed to its attractive material properties, namely, unique shape memory and super-elasticity [22]. On account of these superior material properties, NiTi alloys have been widely used in the biomedical industry for cardiovascular applications, orthopaedic applications and for the manufacture of surgical instrumentation [22,23]. Having said that, NiTi alloys possess a disadvantage in that toxic Ni can be identified within the surface layer [24] and, with the release of Ni into the biological environment, can cause severe negative reactions and biofunctionality [25,26]. In fact, recent work by Sun *et al.* [27] showed that, even at sub-toxic concentrations, Ni ions can give rise to a significant decrease in alkaline phosphatase (ALP) levels as well as hindering DNA synthesis having a negative impact upon cell growth and differentiation. This was further corroborated with the work of Nichols and Puleo [28]. With this major negative impact in mind, surface engineering of NiTi alloys for use as biomaterial is critical to the expansion of the biomaterial industry as it is believed that surface engineering can be applied to reduce the level of Ni release, enhancing the biofunctionality of NiTi alloys [29-32].

It is now common knowledge that the adhesion, proliferation and differentiation of MSCs are highly regulated by micro-environmental and nano-environmental factors such as extracellular matrix (ECM) and substrate surface topography [3,6,33-35]; indeed, it has been identified that MSCs will form different focal attachments on a less organized topographical surfaces and result in a phenotype district [36]. It has been shown that the attachment, adhesion and spreading in the early phase (minutes to hours) of cell-substrate interactions influence the capacity for cell proliferation and to differentiate itself on contact with the implant [37], indicating that the first 24 hours of biological cell growth is crucial. In addition to this, recent research [3,13,38,39] has highlighted that anisotropic laser-induced surface textures can guide cell growth, indicating that surfaces can be fabricated to direct biological cell growth. This also involves cytoskeletal reorganization which is a precondition for MSCs to differentiate into an osteoblastic lineage [40]. On account of this, surface engineering, in particular laser surface engineering, can be seen as an effective means to manipulate the surfaces of biomaterials to give rise to an optimized biomimetic material, enhancing the biological cell response. This enhanced biological cell response, through surface engineering, will then ultimately provide the biomedical industry with a means of developing optimized substrates and scaffolds upon which human tissue can be efficiently grown, especially with consideration of producing optimized substrates and scaffolds on a pharmaceutical scale, meeting the needs of the future with regards to healthcare. This chapter details some of the main surface engineering techniques used for modulating stem cell growth response and details two techniques (laser surface

treatment and laser welding) and the impact these techniques have on stem cell growth and proliferation.

2. Surface Engineering Techniques in Stem Cell Technologies

Since surface engineering has a promising role for the development and optimization of substrates, upon which the growth of biological cells such as MSCs can be enhanced, there is an increasing application of numerous surface engineering techniques to this field [41-45].As a direct result of this, a number of competing techniques have been developed and employed in both academic and industrial environments.

2.1 Laser Surface Engineering

Laser surface engineering has been shown to provide an adequate means of modifying the surfaces of various material types for the sole purpose of surface engineering. That is, the surface topography or surface chemistry (or both simultaneously) can be modified through the application of laser surface engineering [46-48], modulating the biofunctionality of the material [35,49,50]. This is significant as, on numerous occasions, the surface properties of a material give rise to a biological cell response which is inadequate, leading to rejection of the material. This results in minimal, or no, biological adhesion [51].

Another laser material processing technique which has become an attractive means for processing biomaterials is that of laser micro-welding on account of the increasing demand in miniaturized biomedical implant technologies [19,20,52,53].

2.2 Plasma Surface Engineering

Plasma surface engineering has the advantage of being able to manipulate the surface topography and surface chemistry of a material whilst maintaining the initial bulk material properties. As a direct result of this, plasma surface processing has been applied to a number of industries such as healthcare and the automotive industries [54,55]. With specific regard to healthcare and bioengineering it has been widely shown that the implementation of plasma surface engineering has the ability to significantly enhance the biofunctionality of materials, especially with regard to stem cells and influencing their growth and differentiation [56-58].

2.3 Lithography Techniques

Owing to the fact that lithography is a well-established technique, there are a number of variations. Some of the main lithography techniques include photolithography, electron beam lithography, imprint lithography, and dip-pen lithography. Furthermore, due to the advanced nature of this technology, it holds the ability to readily produce surfaces on a nanometre scale which is ideal for the effective control of adhesion and wettability characteristics [59-61]. The main technique used for nano-lithography is that of photolithography which shows significant promise in the manipulation of stem cell growth and differentiation [62,63]. Having said that, it should be noted that for this particular technique to be effective a completely flat material surface is needed, in addition to the necessity of extremely clean operating conditions. This causes implications in terms of both pre- and post-processing leading to significantly high operating costs compared to other competing techniques.

2.4 Micro- and Nano-Printing

Micro- and nano-printing provides a low cost option to efficiently produce engineered polymeric and metal surfaces on a large scale [64-68]. This technology has, therefore, been tipped as one to provide sufficient expansion in healthcare bioengineering industries. Leading on from this, it has

been shown that the adhesion, proliferation and differentiation of pluripotent stem cells can be manipulated through the means of micro- and nano-printing of the substrates on which they are cultured [42]. This is highly significant as it could provide an effective and large-scale technological solution to manufacturing optimised substrates which can be implemented to provide the industry with tailored stem cell growth for use within implant technologies and stem cell therapies.

3. Laser Surface Engineering of Polymeric Materials

3.1 Experimental Technique

3.1.1 Materials

Polyamide 6,6 was sourced in 100 x 100 mm^2 sheets with a thickness of 5.0 mm (Goodfellow Cambridge, Ltd, UK). Polytetrafluoroethylene (PTFE) was sourced in a 500 x 500 mm^2 sheet with a thickness of 0.6 mm. Both polymeric materials were mechanically cut into 10.0 mm diameter samples for CO_2 laser processing, topography analysis, surface chemistry analysis and wettability analysis. Smaller samples with a diameter of 5.0 mm were mechanically cut for biological analysis.

3.1.2 Laser Surface Engineering Techniques

Both the polyamide 6,6 and PTFE were processed using a CO_2 laser marking system (60W Ti-series, Synrad Inc., USA). Further details of the laser set-up can be found in [4,69]. For the polyamide 6,6 samples, the laser-induced patterns were trenches with 50 µm spacing (NT50), hatches with 50.0 µm spacing (NH50), trenches with 100 µm spacing (NT100) and hatches with 100 µm spacing (NH100). For the PTFE samples, the laser-irradiated patterns were 50.0 µm Hatch (PH50), 50.0 µm Trench (PT50), 100 µm Hatch (PH100), and 100.0 µm Trench (PT100). For each of the polyamide 6,6 samples the laser power was kept constant at 11.7% (7 W) with a scanning speed of 600 mms^{-1}. For the PTFE samples, a laser scan speed of 400 mm/s, with 50% power was used. These samples are denoted as "_1" (for example PT100_1). A speed of 600 mm/s, with 28% power was also used and these samples are denoted as "_2" (for example PT100_2). In addition, an as-received control sample (AR) was used.

3.1.3 Analytical Techniques

Surface profiles of each sample were determined using a non-contact confocal chromatic imaging (CCI) system (Micromesure 2; STIL S.A., France) with Surface Map software and TMS Plus software. Further details of this system can be found in [12].

A sessile drop goniometer (OCA20; DataPhysics Instruments GmbH, Germany) was used with SCA20 software to allow the contact angle, θ, for triply distilled water and diiodomethane to be determined for each sample. Before measurement, the samples were cleaned using ethanol in an ultrasonic bath for 10 minutes. Following this the samples were air dried for 30 minutes. An average droplet volume of 5 µl was used for the measurement of the distilled water contact angle, θ, while for the diiodomethane the average droplet volume was 1 µl in order to provide a sufficient size droplet to take measurements. By using the data obtained for the contact angles of the water and the diiodomethane, the two-liquid Owens, Wendt, Rabel and Kaelble (OWRK)method was used to determine the surface free energy for each of the samples.

X-ray photoelectron spectroscopy (XPS) data were acquired using a bespoke ultra-high vacuum system fitted with a monochromatic Al Kα X-ray source (Specs Focus 500, GmbH, Germany), a 150 mm mean radius hemispherical analyser with 9-channeltron detection (Phoibos; Specs GmbH,

Germany), and a charge neutralising electron gun (FG20; Specs GmbH, Germany). Further details of the XPS experimentation are given in [70].

3.1.4 Biological Analysis Techniques

Mesenchymal stem cells (MSCs) used in this study were from human umbilical cord blood (Stem Cell Bank, Japan). The primary MSCs used were at passage number 6. MSCs were grown in tissue culture medium consisting of Dulbecco's Modified Eagles Media (DMEM) (with l-glutamine) (Sigma Aldrich, Ltd., UK), supplemented with 10% fetal calf serum (FCS) (Sigma Aldrich, Ltd., UK), and 100 units/ml of penicillin and 0.1-mg/ml of streptomycin (Sigma Aldrich, Ltd., UK), and placed in an incubator set at 37°C, 5% humidified CO2 (Wolf Laboratories, Ltd., UK), throughout the study. When the cells reached sub-confluence (70 to 80%), they were retrieved with 0.25% trypsin and 0.02% EDTA (Sigma Aldrich, Ltd., UK). The retrieved cells were washed twice with phosphate buffer saline (PBS), centrifuged at 1200 rpm for 12 minutes at room temperature and re-seeded onto the samples which had been placed in the 24- and 96-well plates (Corning Costar; Sigma-Aldrich, Ltd., UK). A consistent sample size of 5×10^4 cells/ml was used throughout the *in-vitro* experiments. Further details with regards to MSC preparation, growth and retrieval are provided in [4].

The cell morphology on different samples after 24 and 48 hours of culture was analysed in the secondary electron (SE) mode by the SEM. The following procedure was undertaken to produce a sample that was dehydrated and ready for Au coating. After removal of the culture medium, the samples were initially rinsed with PBS (Sigma-Aldrich, Ltd., UK) to remove any unattached cells and then adhered cells were fixed using 1.2% glutaraldehyde in water (Sigma-Aldrich, Ltd., UK) at room temperature for an hour within the biological safety cabinet (BSC). After an hour, the glutaraldehyde solution was removed and the fixed cells were washed with PBS prior to carrying out a graded series of ethanol:distilled water mixtures of 50:50, 80:20, 90:10, 95:5, 98:2 and 100:0. Each sample was left in these mixtures for 10 minutes and dried in air. The samples were sputter coated with Au for cell morphology observation by SEM.

3.2 Effects of Laser Surface Engineering on Surface Topography

It is well known and accepted that with an incident infra-red (IR) laser such as a CO_2 laser the coupling of the laser light into the material is that of a thermolytic nature [71], resulting in lattice vibrations and a rise in material temperature. As a result of this, in many cases for CO_2 laser material processing, the rise in temperature gave rise to melting of the material. Some typical three-dimension (3-D) profiles of the polyamide 6,6 samples which have undergone CO_2 laser surface engineering detailed in Section 2 are shown in Figure 1. This highlights that the scanning of the CO_2 laser beam across the polymeric samples gave rise to an increase in surface roughness. That is, the CO_2 laser surface engineering gave rise to an increase in maximum peak heights from approximately 0.5 µm to 44.0 µm. On account of this, the surface roughness increased with a maximum Ra of 4.4 µm.

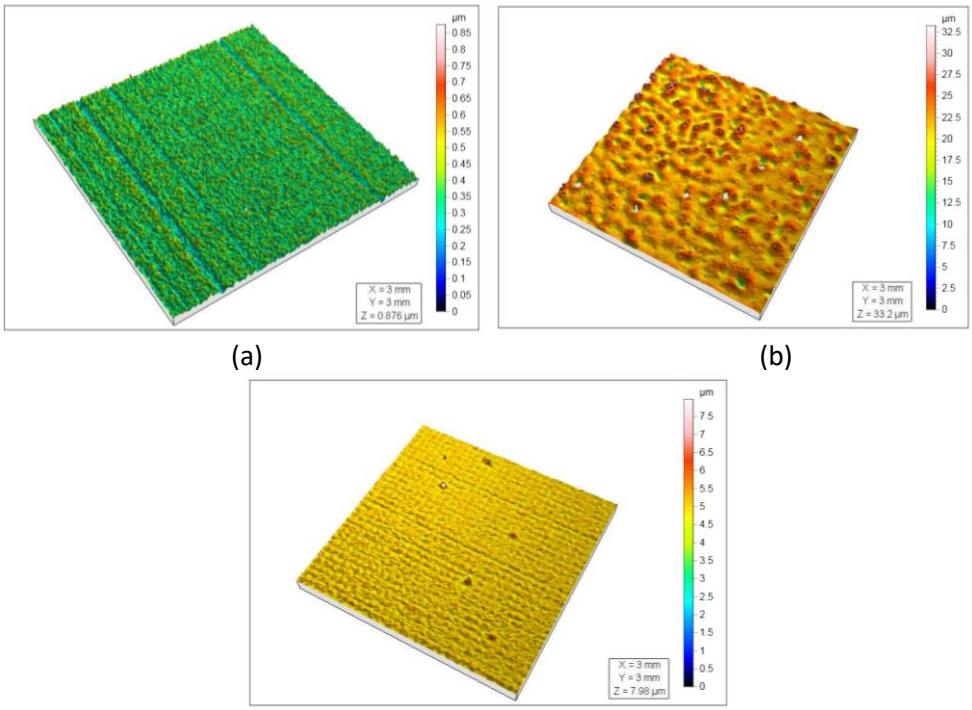

Figure 1: Typical 3-D profiles of (a) the as-received polyamide 6,6 and the CO_2 laser surface engineered polyamide 6,6 – (b) NH50 and (c) NH100 samples.

In a similar fashion, typical 3-D profiles of the CO_2 laser surface engineered PTFE samples are shown in Figure 2 further indicating that the laser surface engineering gave rise to an increase in surface roughness. It should be noted that the highest increase in roughness was approximately double compared to the as-received sample with the largest Ra roughness value being 4.09 µm for sample PH100_2. Still, it was found that the Ra roughness values decreased for the 50 µm spaced PTFE samples in comparison to the as-received sample (see Table 2). In addition to this, it was also observed that for the polyamide 6,6 samples the intended laser-induced scanned pattern was somewhat eradicated during the processing of the 50.0 µm spaced samples. This is of significance as it indicates that, with the laser focussed beam spot being of the order of 95.0 µm, the scanned laser lines across the surface would have overlapped, effectively re-melting sections of the sample. This appears to have reduced the surface roughness of these PTFE samples and eradicated the intended pattern for the nylon 6,6 samples on account of the material properties defining the way in which they reacted to the laser re-melting.

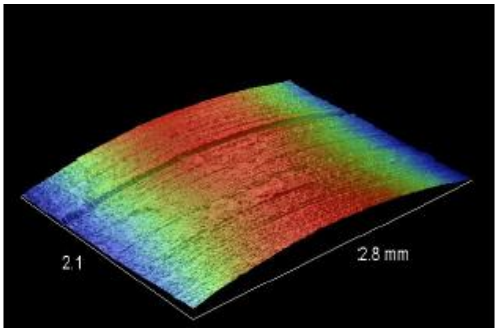

(a)

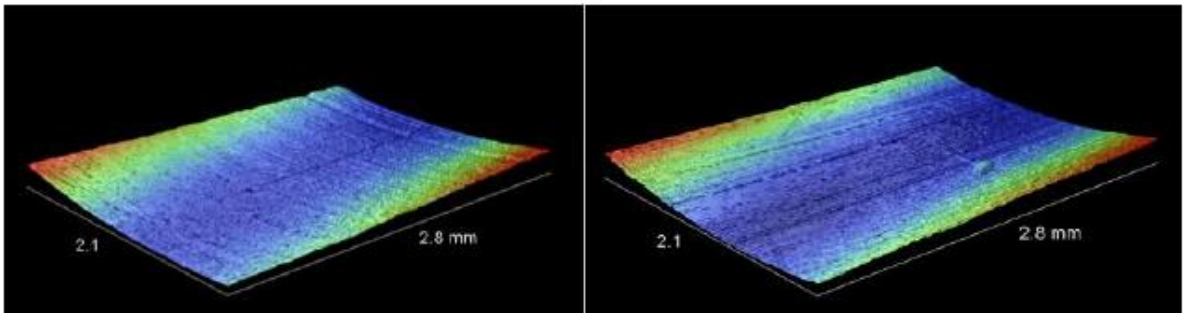

(b) (c)

Figure 2: Typical 3-D profiles of (a) the as-received PTFE sample (PAR) and the CO_2 laser surface engineered PTFE – (b) PT50 and (c) PH100.

Provided in Table 2 are the surface roughness Ra parameters for each surface. It should be noted that for the polyamide samples, the samples which had laser scan dimensions of 50.0 µm gave higher Ra roughness values compared to those samples which underwent 100.0 µm laser scan dimensions. In a similar manner, it was found for some of the 50.0 µm dimension laser scan samples that the Ra roughness value was lower than the other laser surface engineered PTFE samples, including the as-received sample. As discussed previously, it is highly likely that this is due to the overlapping nature of laser beam as it scanned across the surface coupled with the different material properties defining the surface topography outcome during the laser re-melting process.

Table 2: Table showing roughness, contact angle and the corresponding surface free energy for each polymeric sample.

Sample	Ra (μm)	Contact Angle (°) Water	Contact Angle error (°) Water	Surface free Energy (mJm^{-2})
NAR	0.023	56.4	1.29	49.12 ± 0.55
NT50	2.230	60.3	1.72	47.59 ± 0.44
NT100	0.115	55.2	0.81	47.16 ± 0.42
NH50	0.798	54.7	1.06	48.77 ± 0.45
NH100	0.080	57.4	0.61	52.18 ± 1.22
PAR	1.991	91.4	2.05	28.35 ± 1.27
PT50_1	0.354	151.8	1.41	0.94 ± 0.25
PT50_2	3.440	109.6	2.57	1.58 ± 0.03
PH50_1	0.543	147.5	0.19	1.58 ± 0.03
PH50_2	4.250	107.2	0.91	1.58 ± 0.03
PT100_1	1.070	140.4	1.43	3.20 ± 0.38
PT100_2	3.400	117.0	1.93	13.15 ± 1.03
PH100_1	2.500	148.1	0.33	1.48 ± 0.06
PH100_2	4.090	101.5	1.12	22.16 ± 0.68

3.3 Effects of Laser Surface Engineering of Polymeric Materials on Stem Cell Adhesion and Growth

Table 2 provides the contact angle, θ, data for all samples, and the corresponding surface free energy for each sample obtained from goniometer contact angle analysis. As one can see, for the polyamide 6,6 samples, the modification in θ and surface free energy following CO_2 laser surface engineering is minimal with variations in θ ranging from 1.0 to 5.0°. This is contrasted with the PTFE samples which showed a significant increase in θ with contact angles increasing by over 50.0°, making the PTFE samples borderline superhydrophobic (θ>150°). With regards to the polyamide 6,6 samples, it has been shown that CO_2 laser surface engineering can be used to bring about discrete variations in the contact angle and the surface free energy, through topography and surface chemistry modification, discretely modifying the adhesion characteristics. Further details with regards to the manipulation of wettability and adhesion characteristics are given in [72].

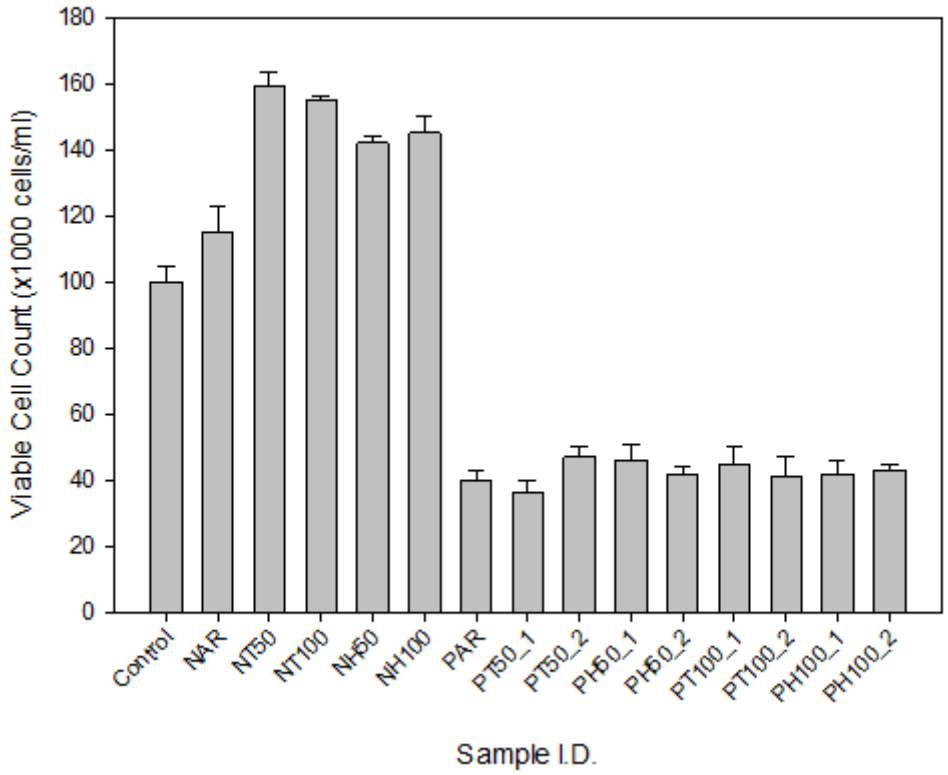

Figure 3: A graph showing the viable cell count for each sample.

As shown in Figure 3, the stem cell growth on the CO_2 laser patterned polyamide 6,6 samples was significantly enhanced compared to the growth on the as-received sample and control sample, following 24 hours of incubation. This is contrasted somewhat with that of the CO_2 laser surface engineered PTFE samples which did not seem to elicit a significant variation in stem cell adhesion and growth. That is, in general for the PTFE samples, the viable cell count following 24 hours incubation remained somewhat constant with viable cell counts being of the order 40,000 cells/ml. This is significant as it is stated by some researchers that highly hydrophobic materials, with high values of θ, hinder the adhesion and growth of biological cells [15]. Having said that, with the added complexity of CO_2 laser processing, it is highly likely that the increase in surface roughness and increase in surface oxygen content could have given rise to a more enhanced response from the stem cells, as has been discussed previously [4,12]. This is in accord with other researchers [15,73,74] and explains the enhanced stem cell response to the CO_2 laser surface engineered polyamide 6,6 samples and the CO_2 laser surface engineered PTFE samples, even considering that the PTFE laser engineered samples are borderline superhydrophobic (θ>150°). Leading on from this, Biazar *et al.* [75] showed that there was a significant relationship between increased surface roughness and enhanced cellular adhesion and cellular spreading. Whilst there seemed to be little variation in cell spreading throughout the CO_2 laser engineered samples, it should be noted that, for the polyamide samples especially, there was an enhancement of stem cell adhesion and growth (see Figure 4 for a typical SEM micrograph of the stem cells adhered to a CO_2 laser engineered polyamide sample).

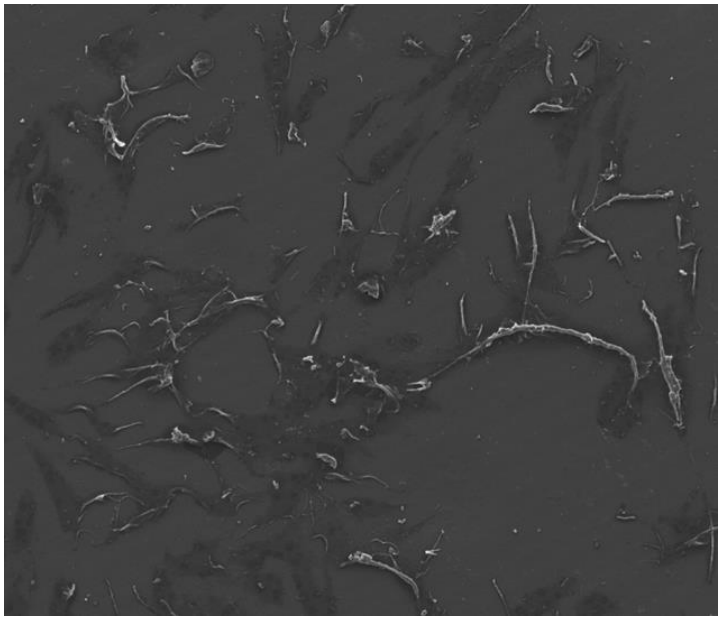

Figure 4: SEM micrograph of typical MSCs growth on Sample NH100 following 24 hours of incubation.

4. Laser Welding of NiTi Alloys

4.1 Experimental Technique

4.1.1 Material

NiTi alloy was sourced flat annealed Ti-55.91 wt. % Ni foil (Johnson Matthey Inc., USA) with dimensions of 50x50x0.25 mm. The material was prepared by removing the oxide layer using 600 grit SiC paper. Following this, all samples were degreased by ultrasonic cleaning for 10 minutes in isopropanol (Sigma Aldrich Inc., USA) and then for 5 minutes in distilled water (Sigma Aldrich Inc., USA). It should be noted that all samples were air dried prior to laser welding.

4.1.2 Laser Micro-Welding Technique

To produce laser autogenous welds, a 100 W, 1091 nm wavelength fibre laser was used, along with an *x-y-z* welding jig to manipulate the movement of the workpiece. In order to minimize the effects of thermal distortion, the welding jig enabled clamping of the samples. To eradicate the possibility of a plasma forming over the weld zone (WZ) argon was used as a shielding gas during the laser welding process. The argon was delivered to the workpiece as a central jet stream through the laser nozzle which had a diameter of 10 mm. It should also be noted that argon was delivered with a side jet with a 6.0 mm diameter output nozzle angled at 30° to the horizontal plane. Previous optimization of the laser welding process had been carried out [76] with the laser power set to 70 W, the welding speed being 300 mm/min, the laser focal position being 1.6 mm from the sample surface and the argon gas flow being 35 l/min.

4.1.3 Analytical and Biological Analysis Techniques

For each sample the Ra surface roughness parameter was defined using a white light interferometer (WLI) (NewView 500, Zygo Ltd., UK). The WLI was set up using a ×50 Mirau lens (NA=0.55) with working distance of 3.4 mm. The Ra and maximum peak-to-valley height roughness parameters for each sample were determined using the MetroPro Software.

The surface chemistry composition of each sample surface was analysed by X-ray photoelectron spectroscopy (XPS) (PHI5600, Physical Electronics Inc., USA). The X-ray source was monochromatic Al K α (15 kV, 25 W) and the beam size was 100 μm in diameter. The pass energies for survey scan and narrow scan spectra were 187.5 and 58.7 eV, respectively.

For the biological analysis, single-tack laser weldments were used which comprised of the weld zone (WZ), the heat affected zone (HAZ) and the base material (BM). The mesenchymal stem cells (Stem Cell Bank, Japan) were grown in tissue culture medium consisting of DMEM (with L-glutamine) (Sigma Aldrich, Ltd.), supplemented with 10% fetal calf serum (FCS) (Sigma Aldrich, Ltd.), and 100 units/ml of penicillin/and 0.1-mg/ml of streptomycin (Sigma Aldrich, Ltd.), and placed in an incubator set at 37°C, 5% humidified CO_2 (Wolf Laboratories, Ltd.), throughout the study. When the cells reached subconfluence (70 to 80%), they were retrieved with 0.25% trypsin and 0.02% EDTA. The retrieved cells were washed twice with PBS, centrifuged at 1200 rpm for 12 minutes at room temperature and re-seeded into four 24-well cell culture plates at an initial seeding density of 5×104 cells per well, and placed in a CO_2 incubator for 24 hours.

Following the 24 hour incubation period, the morphology of the stem cells was analysed by secondary imaging SEM. In order to conduct such an observation the samples were initially rinsed with phosphate-buffered saline (PBS) (Sigma-Aldrich, Ltd.) to remove any unattached cells and then adhered cells were fixed using 1.2% glutaraldehyde in water (Sigma-Aldrich, Ltd.) at room temperature for 1 hour within the BSC. After an hour, the glutaraldehyde solution was removed and the fixed cells were washed with PBS prior to carrying out a graded series of ethanol:distilled water mixtures of 50:50, 80:20, 90:10, 95:5, 98:2 and 100:0. Each sample was left in these mixtures for 10 minutes and dried in air. The samples were sputter coated with Au for cell morphology observation by SEM. The cell coverage (or cover density *per* cm^2) was determined by analyzing the cell coverage on each sample using SEM and optical micrographs with the ImagePro software. The optical micrographs were obtained using an upright optical microscope (Flash 200 Smartscope; OGP Ltd., UK) with magnifications varying between ×100 and ×500.

The number of viable cells on each sample was counted in a 25-square of the haemocytometer (Neubauer Improved Bright Line at depth 0.1 mm, 0.00025 mm^3). Trypan blue was used as the dye to stain the cells. 50 μl of homogeneous cell suspension in tissue culture medium consisting of DMEM (with L-glutamine) (Sigma Aldrich, Ltd., UK) supplemented with 10% fetal calf serum (FCS) and 100 units/ml of penicillin and 0.1 mg/ml of streptomycin (Sigma Aldrich, Ltd., UK) was added to 50 μl of 0.4% trypan blue (Sigma Aldrich, Ltd. UK). This was repeated for two chambers and the mean number of viable cells was obtained, and the following equation was applied: Number of cells /ml=mean number of cells x2 (dilution factor) $x10^4$.

4.2 Surface Chemistry of Laser Micro-Welded NiTi Alloys

Table 3 gives the relative percentages (at.%) for the main metallic elements which were present in the oxide layer following the laser welding process. It should be noted that from the XPS analysis, the Ni at the surface was mainly composed of $Ni(OH)_2$ with a small amount of NiO and metallic Ni. Furthermore, as Table 3 suggests, there was a large concentration of carbon (C) due to environmental contamination. Another interesting factor is that of the Ni/Ti ratio as given in Table 3. The laser welded zone (WZ) gave rise to the lowest Ni/Ti ratio of 0.10 with the ratio increasing over the heat affected zone (HAZ) and the base material (BM). This is highly significant as it is known that the Ni/Ti ratio can provide an indication as to the potential levels of Ni release when used as an implant in a biological environment [77]. With this in mind, due to the low Ni/Ti ratio established by the laser welding process, it is highly likely that this would give rise to enhanced biomimetic properties, making the NiTi alloy material safer for implantation, reducing the probability of Ni release.

Table 3: Surface atomic composition and the surface roughness parameters for the various weldment regions.

Region	C (at.%)	N (at.%)	Ni (at.%)	O (at.%)	Ti (at.%)	Ni/Ti Ratio	Ra (μm)	Max. Peak-to-valley height (μm)
WZ	33.0	1.8	1.5	48.1	15.6	0.10	0.375	2.49
HAZ	35.1	3.1	2.2	44.7	14.9	0.15	0.289	1.46
BM	36.9	2.6	2.6	43.6	14.3	0.18	0.301	1.53

4.3 Effects of Laser Welding of NiTi Alloy on Stem Cell Adhesion and Growth

SEM micrographs of stem cells attaching to the laser welded NiTi alloy and the base material are shown in Figure 5. This shows that the stem cells successfully adhered to the samples with the pseudopodia stretching out over the sample surfaces to assist in further proliferation. It was also observed that stem cells appeared to preferentially adhere to laser-induced surface features indicating that the stem cells preferentially adhered to those surfaces with high, irregular surface roughness. This is in agreement with what has been observed previously by other researchers [15,36,42,43,62]. In addition, it was identified, with the stem cells being sensitive to surface features, that the stem cells were somewhat guided during the 24 hour incubation period. This is owing to the fact that the stem cells appeared to grow in correspondence with the dendritic pattern associated with the laser welded NiTi alloy [3], especially on the rougher surface with the highest maximum peak-to-valley height (see Table 3). This is likely on account of the pseudopodia playing a nano-scale sensory role for guiding and manipulating the stem cell adhesion, growth and proliferation [78]. It has also been shown by other researchers that the larger the surface features, the higher the degree of direct guided cell growth, depending on the cell type [79]. Therefore, for stem cell technologies which require directed and guided cellular growth, it is highly advisable that the surface engineering technique should be chosen to augment the maximum peak-to-valley height roughness parameter.

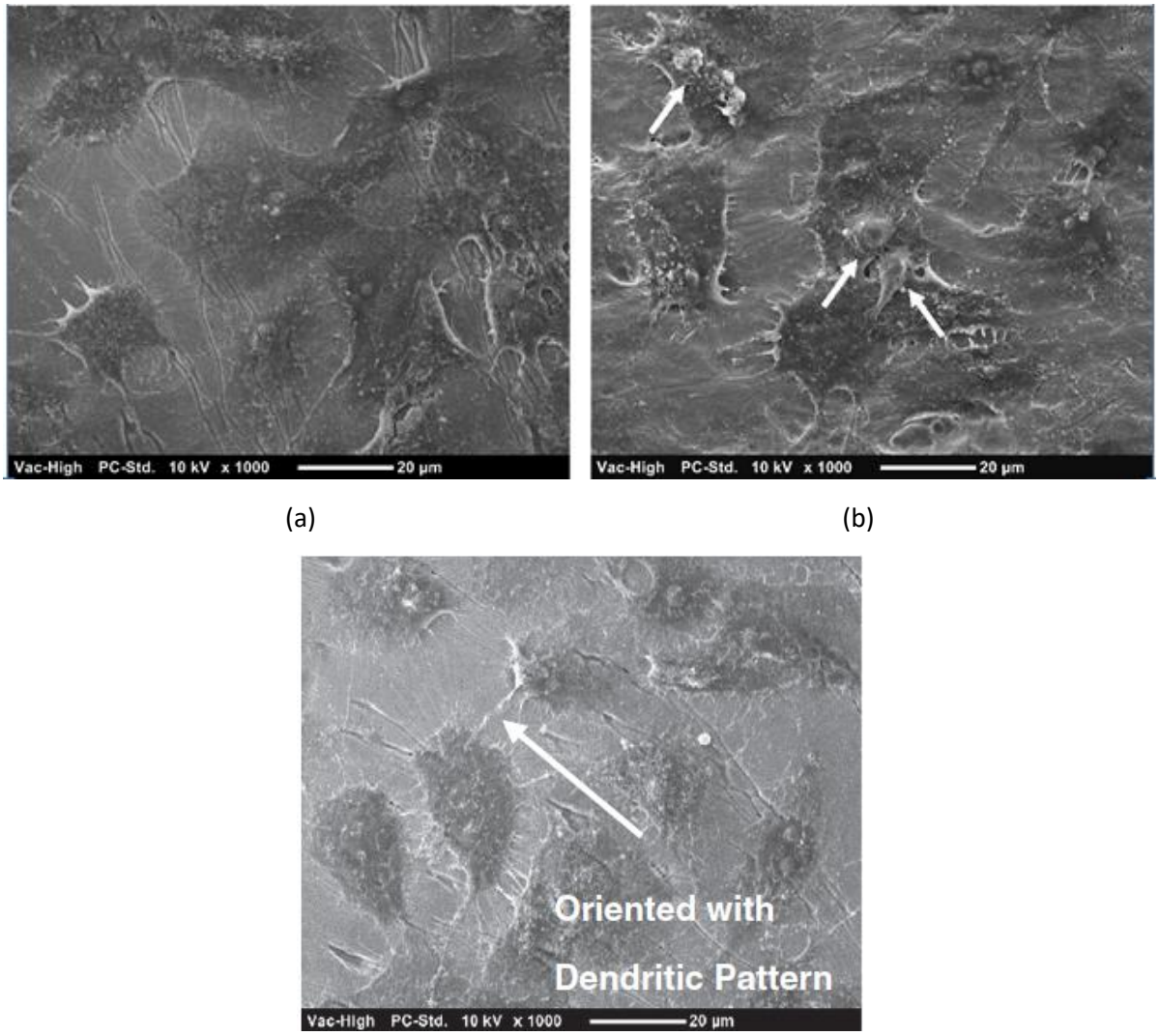

Figure 5: SEM micrographs of the stem cells adhering and growing on (a) laser welded NiTi alloy (WZ) and (b) the base material (BM) with white arrows identifying that some cells have kept there round morphology and (c) laser welded NiTi alloy showing the oriented cell growth with a dendritic pattern.

The percentage coverage of the stem cells over the NiTi alloy samples is shown in Figure 6. It should be noted that the laser welded NiTi alloy (WZ) gave rise to the highest stem cell coverage of 86% compared to the HAZ and BM giving rise to 73% and 76%, respectively. This further indicates the importance of surface roughness and surface features with regards to manipulating stem cell adhesion and proliferation. That is, the cell coverage appears to be somewhat related to the laser-induced surface roughness, with rougher surfaces corresponding to higher cell coverages. This is further in agreement with other researchers who have found that anchorage dependent cells preferentially grow and proliferate on rougher surfaces [80,81]. This is owing to the fact that the rougher surfaces give rise to an increased surface area with which the biological cells can interact [17]. With regards to the stem cells, it may also have been the case that the laser-induced dendritic pattern improved the cytoskeleton, in accord with Eisenbarth *et al.* [82] who showed that oriented and guided cells have a higher density of focal contact in the regions of induced surface patterns. In addition to this, the higher cell coverage for the laser welded samples could very well be augmented by the low Ni/Ti ratio which is known to assist in the formation of a passive film, with a higher concentration of TiO_2.

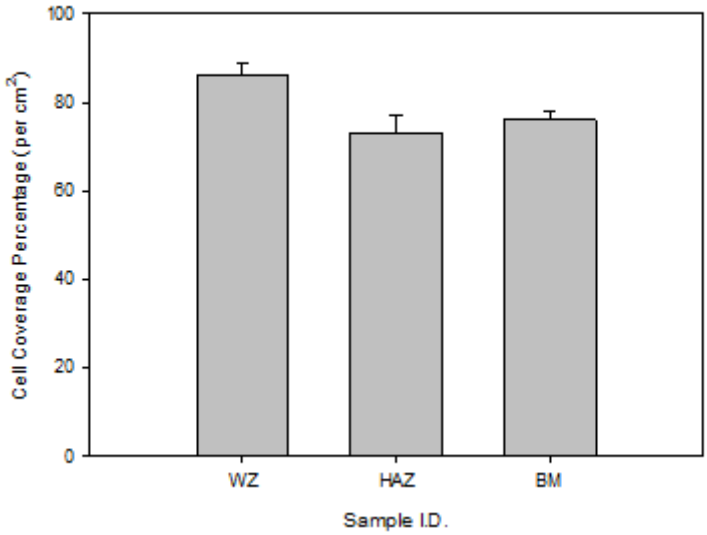

Figure 6: Graph showing the stem cell coverage for each sample following 24 hours incubation.

The viable cell count for the NiTi alloy samples, in comparison with the polyamide 6,6 samples and the PTFE samples, is shown in Figure 7. With regards to the NiTi alloy samples, it was found that the laser welded sample (WZ) gave rise to an increase in viable cell count compared to the HAZ and BM. This corresponds to what was identified with the stem cell coverage shown in Figure 6. Furthermore, it should be noted that after 24 hours of incubation, the NiTi alloy samples promoted stem cell growth and proliferation considerably more compared to the polymeric samples (polyamide 6,6 and PTFE). This indicates that the NiTi alloy is sufficiently more biocompatible compared to the polymeric materials and explains why, currently, NiTi alloy is more widely used in the biomedical industry. Having said that, with the polyamide 6,6 showing potential for enhanced stem cell growth, from laser surface engineering, it is likely that the biomedical industry would be interested in such technologies to manipulate cheaper materials which can be easily modified. Having said that, considerably more research is needed into the manipulation of stem cells through surface engineering and with the significant advancements in surface engineering techniques it is highly likely that within the next 10 to 20 years surface engineering will be used in the mainstream biomedical industries as a way to manipulate and dictate biological cell growth.

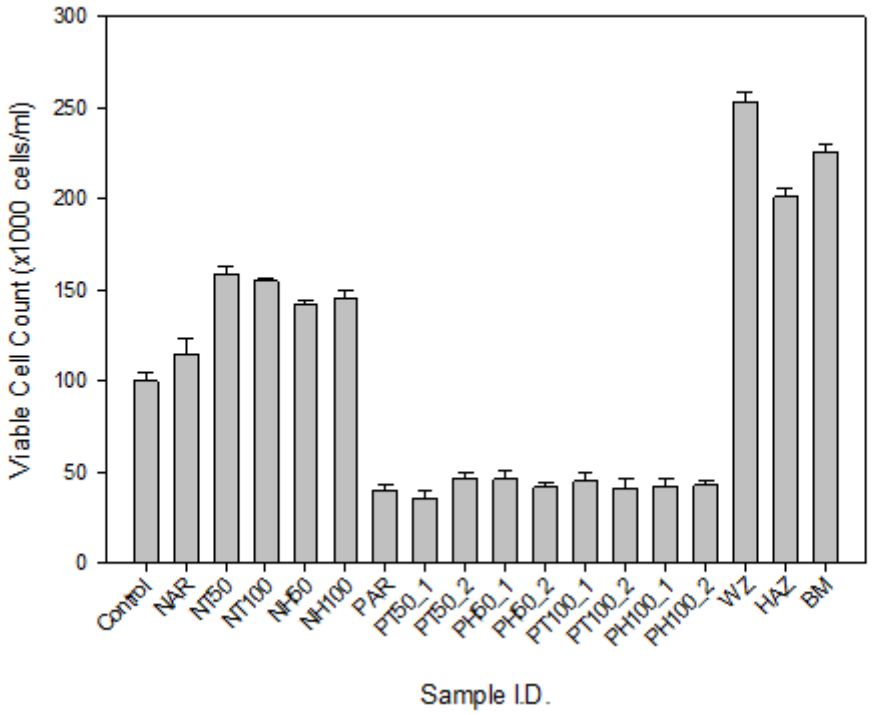

Figure 7: Graph showing the viable cell count for the polyamide 6,6 samples, PTFE samples and the NiTi samples (WZ, HAZ and BM).

5. Summary and Future Considerations

With an ageing worldwide population following an upward trend it is becoming significantly evident that there are numerous socio-economic implications which need to be counteracted, this is especially the case for the healthcare industry. As a direct result of this numerous surface engineering techniques have been developed to provide a means to modify the surfaces of biomaterials to manipulate the growth of biological cells. This chapter has discussed some of the main engineering techniques and has shown how laser material processing in the form of laser surface engineering and laser welding can be implemented to ensure that stem cell adhesion, growth and proliferation can be enhanced simply by discretely and simultaneously modifying the surface roughness and surface chemistry of distinctly different ,materials: polymeric materials and NiTi alloys, to yield the same positive effect. Given the wide selection of lasers available in the market today it is safe to say that almost every material can be processed using laser technology. This can potentially open up a large array of applications for different materials in the biomedical and healthcare industries and could lead to further expansion, enhancing technologies and therapies.

The work presented herein has shown that both the modifications in surface topography and surface chemistry have a considerable impact upon stem cell adhesion, growth and proliferation. It has been evidenced that there is a significant relationship between the roughness of a material and the growth of the stem cells. For the polymeric materials, it was shown that there was an enhanced stem cell response with an increase in roughness and increase in surface oxygen content. Having said that, for those PTFE samples which evidenced a near superhydrophobic surface ($\theta>150°$), there

appeared to be no variation in stem cell response when compared to the as-received sample. This is of significance as it shows that samples with a high contact angle, following laser surface engineering, could still be implemented for use in the healthcare industry for stem cell growth. Through further research this type of surface may be beneficial for complex biological environments, hindering bacterial growth whilst keeping the stem cell adhesion, growth and proliferation at as-received levels. For the NiTi alloy it has also been shown that laser micro-welding is likely to give rise to a surface which would release less Ni into a biological environment, making it less toxic and more biomimetic.

With specific regard to stem cells, it has been shown that the use of a CO_2 laser for surface engineering of polyamide 6,6 can give rise to an enhanced stem cell growth, giving an increase of 35% in viable cell count compared to the as-received sample. What is more, through fiber laser autogenous welding of NiTi alloy, it has been shown that the stem cell adhesion, growth and proliferation can be enhanced by increasing both the percentage cell coverage and viable cell count. This is significant as it shows that laser micro-welding could be implemented in the manufacture of biological implants whilst enhancing the biomimetic nature of the material at the same time.

7. References

1. K. Anselme, P. Davidson, A.M. Popa, M. Giazzon, M. Liley and L. Ploux, The interaction of cells and bacteria with surfaces structured at the nanometre scale. *Acta Biomaterialia* 6, 3824-3846 (2010).

2. P. Evers, *The Global Market for Stem Cells*. BCC Research BIO035F, Wellesley, MA, USA (2016).

3. C.W. Chan, I. Hussain, D.G. Waugh, J. Lawrence and H.C. Man, Effect of laser treatment on the attachment and viability of mesenchymal stem cell responses on shape memory NiTi alloy. *Mater. Sci. Eng. C* 42, 254-263 (2014).

4. D.G. Waugh, I. Hussain, J. Lawrence, G.C. Smith, D. Cosgrove and C. Toccaceli, In vitro mesenchymal stem cell response to a CO2 laser modified polymeric material. *Mater. Sci. Eng. C* 67, 727-736 (2016).

5. A. Carre and K.L. Mittal (Eds.) *Surface and Interfacial Aspects of Cell Adhesion*. CRC Press, Boca Raton, FL, USA (2011).

6. L.E. McNamara, R.J. McMurray, M.J. Biggs, F. Kantawong, R.O. Oreffo and M.J. Dalby, Nanotopographical control of stem cell differentiation. *J. Tissue Eng.* Article ID 120623 (2010).

7. W. Wang, K. Kratz, M. Behl, W. Yan, Y. Liu and X. Xu, The interaction of adipose-derived human mesenchymal stem cells and polyether ether ketone. *Clinical Hemorheology Microcirculation* 61, 301-321 (2015).

8. W. Tsuji, J.P. Rubin and K.G. Marra, Adipose-derived stem cells: Implications in tissue regeneration. *World J. Stem Cells* 6, 312-321 (2014).

9. H. Koga, L. Engebretsen, J.E. Brinchmann, T. Muneta and I. Sekiya, Mesenchymal stem cell-based therapy for cartilage repair: A review. *Knee Surgery, Sports Traumatology, Arthroscopy: Official J. ESSKA* 17, 1289-1297 (2009).

10. M.G. Angelos and D.S. Kaufman, Pluripotent stem cell applications for regenerative medicine. *Current Opinion Organ Transplantation* 20, 663-370 (2015).

11. R.S. Mahla, Stem cells applications in regenerative medicine and disease therapeutics. *Int. J. Cell Biology* Article ID 6940283 (2016).

12. D.G. Waugh and J. Lawrence, CO2 laser surface patterning of nylon 6,6 and subsequent effects on wettability characteristics and apatite response. *Surf. Eng.* 27, 724-728 (2011).

13. D.G. Waugh, J. Lawrence, D.J. Morgan and C.L. Thomas, Interaction of CO2 laser-modified nylon with osteoblast cells in relation to wettability. *Mater. Sci. Eng. C* 29, 2514-2524 (2009).

14. D.G. Waugh, J. Lawrence and E.M. Brown, Osteoblast cell response to a CO2 laser modified polymeric material. *Opt. Lasers Eng.* 50, 236-247 (2012).

15. A.S.G. Curtis and C.D.W. Wilkinson, Reactions of cells to topography. *J. Biomater. Sci. Polym. Ed.* 9, 1313-1329 (1998).

16. C.W. Chan, I. Hussain, D.G. Waugh, J. Lawrence and H.C. Man, In vitro mesenchymal stem cell responses on laser-welded NiTi alloy. *Mater. Sci. Eng. C* 33, 1344-1354 (2013).

17. D.S. Kommireddy, S.M. Sriram, Y.M. Lvov and D.K. Mills, Stem cell attachment to layer-by-layer assembled TiO2 nanoparticle thin films. *Biomaterials* 27, 4296-4303 (2006).

18. A. Sionkowska, Current research on the blends of natural and synthetic polymers as new biomaterials: Review. *Prog. Polym. Sci.* 36, 1254-1276 (2011).

19. Y. Maghdouri-White, G.L. Bowlin, C.A. Lemmon and D. Dréau, Bioengineered silk scaffolds in 3D tissue modeling with focus on mammary tissues. *Mater. Sci. Eng. C* 59, 1168-1180 (2016).

20. A. Kumar, A. Srivastava, I.Y. Galaev and B. Mattiasson, Smart polymers: Physical forms and bioengineering applications. *Prog. Polym. Sci.* 32, 1205-1237 (2007).

21. S.K. Jaganathan, E. Supriyanto, S. Murugesan, A. Balaji and M.K. Asokan, Biomaterials in cardiovascular research: Applications and clinical implications. *Biomedical Res. Intl.* Article ID 459465 (2014).

22. T. Duerig, A. Pelton and D. Stöckel, An overview of nitinol medical applications. *Mater. Sci. Eng. A* 273-275, 149-160 (1999).

23. N.B. Morgan, Medical shape memory alloy applications—the market and its products. *Mater. Sci. Eng. A* 378, 16-23 (2004).

24. S.A. Shabalovskaya and J.W. Anderegg, Surface spectroscopic characterization of TiNi nearly equiatomic shape memory alloys for implants. *J. Vac. Sci. Technol. A* 13, 2624-2632 (1998).

25. A. Kapanen, J. Ryhänen, A. Danilov and J. Tuukkanen, Effect of nickel–titanium shape memory metal alloy on bone formation. *Biomaterials* 22, 2475-2480 (2001).

26. D. Tarnita, D.N. Tarnita, N. Bizdoaca, I. Mindrila and M. Vasilescu, Properties and medical applications of shape memory alloys. *Romanian J. Morphology Embryology* 50, 15-21 (2009).

27. Z.L. Sun, J.C. Wataha and C.T. Hanks, Effects of metal ions on osteoblast-like cell metabolism and differentiation. *J. Biomed. Mater. Res.* 34, 29-37 (1997).

28. K.G. Nichols and D.A. Puleo, Effect of metal ions on the formation and function of osteoclastic cells in vitro. *J. Biomed. Mater. Res.* 35, 265-271 (1997).

29. H.C. Man, Z.D. Cui and T.M. Yue, Corrosion properties of laser surface melted NiTi shape memory alloy. *Scripta Materialia* 45, 1447-1453 (2001).

30. Z.D. Cui, H.C. Man and X.J. Yang, The corrosion and nickel release behavior of laser surface-melted NiTi shape memory alloy in Hanks' solution. *Surf. Coat. Technol.* 192, 347-353 (2005).

31. M.H. Wong, F.T. Cheng and H.C. Man, Laser oxidation of NiTi for improving corrosion resistance in Hanks' solution. *Mater. Letters* 61, 3391-3394 (2007).

32. M.H. Wong, F.T. Cheng, G.K.H. Pang and H.C. Man, Characterization of oxide film formed on NiTi by laser oxidation. *Mater. Sci. Eng. A* 448, 97-103 (2007).

33. J.R. Mauney, V. Volloch and D.L. Kaplan, Role of adult mesenchymal stem cells in bone tissue engineering applications: Current status and future prospects. *Tissue Eng.* 11, 787-802 (2005)

34. D. Khang, J. Choi, Y. Im, Y. Kim, J. Jang and S.S. Kang, Role of subnano-, nano- and submicron-surface features on osteoblast differentiation of bone marrow mesenchymal stem cells. *Biomaterials* 33, 5997-6007 (2012).

35. D.G. Waugh, C. Toccaceli, A.R. Gillett, C.H. Ng, S.D. Hodgson and J. Lawrence, Surface treatments to modulate bioadhesion: A critical review. *Rev. Adhesion Adhesives* 4, 69-103 (2016).

36. J. Lincks, B.D. Boyan, C.R. Blanchard, C.H. Lohmann, Y. Liu, D.L. Cochran and D.D. Dean, Response of MG63 osteoblast-like cells to titanium and titanium alloy is dependent on surface roughness and composition. *Biomaterials* 19, 2219-2232 (1998).

37. M. Stiehler, M. Lind, T. Mygind, A. Baatrup, A. Dolatshahi-Pirouz, H. Li and M. Foss, Morphology, proliferation, and osteogenic differentiation of mesenchymal stem cells cultured on titanium, tantalum, and chromium surfaces. *J. Biomed. Mater. Res.* 86A, 448-458 (2008).

38. C. Liang, H. Wang, J. Yang, B. Li, Y. Yang and H. Li, Biocompatibility of the micro-patterned NiTi surface produced by femtosecond laser. *Appl. Surf. Sci.* 261, 337-342 (2012).

39. A. Cunha, A.P. Serro, V. Oliveira, A. Almeida, R. Vilar and M. Durrieu, Wetting behaviour of femtosecond laser textured Ti–6Al–4V surfaces. *Appl . Surf. Sci.* 265, 688-696 (2013).

40. E.K. Yim, R.M. Reano, S.W. Pang, A.F. Yee, C.S. Chen and K.W. Leong, Nanopattern-induced changes in morphology and motility of smooth muscle cells. *Biomaterials* 26, 5405-5013 (2005).

41. T. Limongi, L. Lizzul, A. Giugni, L. Tirinato, F. Pagliari and H. Tan, Laboratory injection molder for the fabrication of polymeric porous poly-epsilon-caprolactone scaffolds for preliminary mesenchymal stem cells tissue engineering applications. *Microelectronic Eng.* 175, 12-16 (2017).

42. P. Wang, H. Thissen and P. Kingshott, Modulation of human multipotent and pluripotent stem cells using surface nanotopographies and surface-immobilised bioactive signals: A review. *Acta Biomaterialia* 45, 31-59 (2016).

43. W. Chen, Y. Shao, X. Li, G. Zhao and J. Fu, Nanotopographical surfaces for stem cell fate control: Engineering mechanobiology from the bottom. *Nano Today* 9, 759-784 (2014).

44. Y. Zhao, K. Tan, Y. Zhou, Z. Ye and W. Tan, A combinatorial variation in surface chemistry and pore size of three-dimensional porous poly(ε-caprolactone) scaffolds modulates the behaviors of mesenchymal stem cells. *Mater. Sci. Eng. C* 59, 193-202 (2016).

45. K. Cai, M. Lai, W. Yang, R. Hu, R. Xin and Q. Liu, Surface engineering of titanium with potassium hydroxide and its effects on the growth behavior of mesenchymal stem cells. *Acta Biomaterialia* 6, 2314-2321 (2010).

46. K.W. Ng, J. Lawrence, H.C. Man, T.M. Yue and D.G. Waugh, Enhancement of the wettability characteristics of a nickel-titanium (NiTi) medical implant alloy by laser surface alloying with molybdenum (Mo) and niobium (Nb). *Lasers in Engineering* 26, 269-283 (2013).

47. D.G. Waugh and J. Lawrence, *Laser Surface Treatment of a Polymeric Biomaterial: Wettability Characteristics and Osteoblast Cell Response Modulation*. Old City Publishing, Philadelphia, PA, USA (2014).

48. D.G. Waugh and J. Lawrence, The enhancement of biomimetic apatite coatings by means of KrF excimer laser surface treatment of nylon 6,6. *Lasers in Engineering* 21, 95-114 (2011).

49. C. Chen, M. Lee, V.B. Shyu, Y. Chen, C. Chen and J. Chen, Surface modification of polycaprolactone scaffolds fabricated via selective laser sintering for cartilage tissue engineering. *Mater. Sci. Eng. C* 40, 389-397 (2014).

50. R. Kumari, T. Scharnweber, W. Pfleging, H. Besser and J.D. Majumdar, Laser surface textured titanium alloy (Ti–6Al–4V) – Part II – Studies on bio-compatibility. *Appl. Surf. Sci.* 357, 750-758 (2015).

51. D.G. Waugh and J. Lawrence, Laser surface processing of polymers for biomedical applications. In: *Laser-Assisted Fabrication of Materials*, J.D. Majumdar, I. Manna (Eds.), Heidelberg, Berlin, Germany pp. 275-318 Springer Berlin (2012).

52. R. Matta and J.E. Davies, Chapter 11 - Bioengineering and regenerative medicine in surgery. In: *Bioengineering for Surgery,* W.A. Farhat, J. Drake (Eds.), pp. 189-203, Chandos Publishing, Cambridge, UK (2016).

53. M. Rizwan, G.S.L. Peh, H. Ang, N.C. Lwin, K. Adnan and J.S. Mehta, Sequentially-crosslinked bioactive hydrogels as nano-patterned substrates with customizable stiffness and degradation for corneal tissue engineering applications. *Biomaterials* 120, 139-154 (2017).

54. M. Thomas and K.L. Mittal (Eds.), *Atmospheric Pressure Plasma Treatment of Polymers: Relevance to Adhesion*, Wiley-Scrivener, Beverly, MA, USA (2013).

55. M. Strobel, C. Lyons and K.L. Mittal (Eds.), *Plasma Surface Modification of Polymers: Relevance to Adhesion*, CRC Press, Boca Raton, FL, USA (1994).

56. R. Matsumoto, K. Shimizu, T. Nagashima, H. Tanaka, M. Mizuno and F. Kikkawa, Plasma-activated medium selectively eliminates undifferentiated human induced pluripotent stem cells. *Regenerative Therapy* 5, 55-63 (2016).

57. M.F. Griffin, A. Ibrahim, A.M. Seifalian, P.E.M. Butler, D.M. Kalaskar and P. Ferretti, Chemical group-dependent plasma polymerisation preferentially directs adipose stem cell differentiation towards osteogenic or chondrogenic lineages. *Acta Biomaterialia* http://dx.doi.org/10.1016/j.actbio.2016.12.016 (2016).

58. F.R. Pu, R.L. Williams, T.K. Markkula and J.A. Hunt, Expression of leukocyte–endothelial cell adhesion molecules on monocyte adhesion to human endothelial cells on plasma treated PET and PTFE in vitro. *Biomaterials* 23, 4705-4718 (2002).

59. Y.H. Sung, Y.D. Kim, H. Choi, R. Shin, S. Kang and H. Lee, Fabrication of superhydrophobic surfaces with nano-in-micro structures using UV-nanoimprint lithography and thermal shrinkage films. *Appl. Surf. Sci.* 349, 169-173 (2015).

60. T. Kim, C. Min, M. Jung, J. Lee, C. Park and S. Kang, Design methodology for nano-engineered surfaces to control adhesion: Application to the anti-adhesion of particles. *Appl. Surf. Sci.* 389, 889-893 (2016).

61. I. Gnilitskyi, F. Rotundo, C. Martini, I. Pavlov, S. Ilday and E. Vovk, Nano patterning of AISI 316L stainless steel with Nonlinear Laser Lithography: Sliding under dry and oil-lubricated conditions. *Tribology Intl.* 99, 67-76 (2016).

62. Q. Huang, T.A. Elkhooly, X. Liu, R. Zhang, X. Yang and Z. Shen, Effects of hierarchical micro/nano-topographies on the morphology, proliferation and differentiation of osteoblast-like cells. *Colloids Surfaces B* 145, 37-45 (2016).

63. G. Abagnale, M. Steger, V.H. Nguyen, N. Hersch, A. Sechi and S. Joussen, Surface topography enhances differentiation of mesenchymal stem cells towards osteogenic and adipogenic lineages. *Biomaterials* 61, 316-326 (2015).

64. A. Patrascioiu, M. Duocastella, J.M. Fernández-Pradas, J.L. Morenza and P. Serra, Liquids microprinting through a novel film-free femtosecond laser based technique. *Appl. Surf. Sci.* 257, 5190-5194 (2011).

65. I. Zergioti, S. Mailis, N.A. Vainos, A. Ikiades, C.P. Grigoropoulos and C. Fotakis, Microprinting and microetching of diffractive structures using ultrashort laser pulses. *Appl. Surf. Sci.* 138-139, 82-86 (1999).

66. R. Wakamatsu and J. Taniguchi, Nanoscale metal pattern-transfer technique using silver ink. *Microelectronic Eng.* 123, 94-99 (2014).

67. S. Buzzi, F. Robin, V. Callegari and J.F. Löffler, Metal direct nanoimprinting for photonics. *Microelectronic Eng.* 85, 419-424 (2008).

68. C.F. Huang, Y. Lin, Y.K. Shen and Y.M. Fan, Optimal processing for hydrophobic nanopillar polymer surfaces using nanoporous alumina template. *Appl. Surf. Sci.* 305, 419-426 (2014).

69. D.G. Waugh, J. Lawrence, C.D. Walton and R.B. Zakaria, On the effects of using CO2 and F2 lasers to modify the wettability of a polymeric biomaterial. *Opt. Laser Technol.* 42, 347-356 (2010).

70. D.G. Waugh and J. Lawrence, Wettability characteristics variation of nylon 6,6 by means of CO2 laser generated surface patterns. *ICALEO 2008 Proceedings*, Pechanga, CA, USA 101 (2008).

71. V.M. Allmen, *Laser-Beam Interactions with Materials*, Springer, Berlin, Germany (1995).

72. D.G. Waugh, J. Lawrence and P. Shukla, Modulating the wettability characteristics and bioactivity of polymeric materials using laser surface treatment. *J. Laser Applications.* 28, 022502 (2016).

73. H. Mirzadeh and M. Dadsetan, Influence of laser surface modifying of polyethylene terephthalate on fibroblast cell adhesion. *Radiation Phys. Chem.* 67, 381-385 (2003).

74. W. Pfleging, M. Bruns, A. Welle and S. Wilson, Laser-assisted modification of polystyrene surfaces for cell culture applications. *Appl. Surf. Sci.* 253, 9177-9184 (2007).

75. E. Biazar, M. Heidari, A. Asefnezhad and N. Montazeri, The relationship between cellular adhesion and surface roughness in polystyrene modified by microwave plasma radiation. *Int. J. Medicine* 6, 631-639 (2011).

76. C.W. Chan and H.C. Man, Laser welding of thin foil nickel–titanium shape memory alloy. *Optics and Lasers in Engineering* 49, 121-126 (2011).

77. W. Chrzanowski, E.A.A. Neel, D.A. Armitage, K. Lee, W. Walke and J.C. Knowles. Nanomechanical evaluation of nickel–titanium surface properties after alkali and electrochemical treatments. *J. Royal Soc. Interface* 5, 1009-1022 (2008).

78. M.J. Dalby, A. Andar, A. Nag, S. Affrossman, R. Tare and S. McFarlane, Genomic expression of mesenchymal stem cells to altered nanoscale topographies. *J. Royal Soc. Interface* 5, 1055-1065 (2008).

79. L. Ponsonnet, V. Comte, A. Othmane, C. Lagneau, M. Charbonnier and M. Lissac, Effect of surface topography and chemistry on adhesion, orientation and growth of fibroblasts on nickel–titanium substrates. *Mater. Sci. Eng. C* 21, 157-165 (2002).

80. T.P. Kunzler, C. Huwiler, T. Drobek, V. Janos and N.D. Spencer, Systematic study of osteoblast response to nanotopography by means of nanoparticle-density gradients. *Biomaterials* 28, 5000-5006 (2007)

81. C. Wirth, V. Comte, C. Lagneau, P. Exbrayat, M. Lissac and N. Jaffrezic-Renault, Nitinol surface roughness modulates in vitro cell response: A comparison between fibroblasts and osteoblasts. *Mater. Sci. Eng. C* 25, 51-60 (2005).

82. E. Eisenbarth, P. Linez, V. Biehl, D. Velten, J. Breme and H.F. Hildebrand, Cell orientation and cytoskeleton organisation on ground titanium surfaces. *Biomolecular Eng.* 19, 233-237 (2002).